Liquid Sensors Based on Enhanced Fabry–Perot Etalons

Nezam Uddin, Maheshwar Shrestha, Bocong Zheng, Hyeun-Joong Yoon, Xiuqing Wang, and Qi Hua Fan

***Abstract*— An optically enhanced Fabry–Perot etalon was demonstrated to accurately measure the refractive index of sugar solutions. The etalon consisted of two silver/SiO_2-coated glass substrates separated by a spacer. The semi-transparent silver films of ∼ 15-nm thickness greatly enhanced the interference of light. The SiO_2 layer coated on the silver created a hydrophilic surface in addition to protecting the silver from oxidation. The hydrophilic behavior of the SiO_2 films together with a capillary action allowed the tested liquids to easily flow into and wet the cavity between the two pieces of glass. Optical spectrophotometer was used to measure the transmission spectra of the etalon with and without a sugar solution. The refractive indices of sugar solutions with different brix concentrations were subsequently determined from the interference peak positions. The results showed a linear response of the refractive index to the brix concentration with a ratio of ∼ 1.7×10^{-3} refractive index per brix%, making the etalons promising for analyzing specific chemicals in liquids.**

***Index Terms*— Sugar solution, Fabry-Perot etalon, liquid sensor, refractive index, hydrophilic.**

I. Introduction

ACCURATE measurement of glucose level in blood is essential for the diabetic patients. The current glucose meters still need improvement in accuracy. On the other hand, there is a relationship between the state of human biological systems and the refractive index of constituent fluids, such as glucose level in blood [1]. Previous research confirmed that the glucose levels could be determined by the refractive index of blood [2], [3]. Therefore, optical spectroscopy is potentially accurate to measure glucose concentration because a small change in the refractive index can be directly detected from optical interference. This concept has stimulated great research interests.

Chong *et al.* demonstrated a refractometer based on a long-period-grating fiber to measure the refractive index of sugar solutions [4]. Devices based on surface plasmon resonance [5], [6] or using optical fiber [7]–[10] were also reported, showing promising results in detecting the sugar levels in water solutions. Optical means of refractive index measurement using surface plasmon resonance (SPR), total internal reflection (TIR) and leaky mode also have demonstrated potential applications in biological field. In TIR measurement, the evanescent field intensity decreased along the depth of the sensing medium when the light wave propagated at an interface. Hence, the optical interaction was weak as merely few percent of the energy propagated in the sensing medium surface [11]. In SPR measurements, metal layers were used in the sensing surface. The sensitivity of SPR sensors was somewhat limited due to the wide resonance dip in the reflection spectrum as light passed through a lossy metal layer (higher k value) [12]. Different approaches have been used to improve the sensitivity and light-matter interaction. A porous layer and nanoparticle assembly could increase the light-matter interaction [13], while a leaky mode was used to measure high refractive index materials by including the entire particle interactions within the evanescent field of the sensors. In these methods, either the devices require nanofabrication processes that are currently expensive or the signal intensity needs to be improved.

Fabry-Perot etalons have been demonstrated to be potentially simple and accurate for measuring the refractive index of liquids [14]–[16]. Most of the Fabry-Perot-type sensors for detecting chemical or biological substances in liquids were based on optical fibers [17], in which the interference occurred due to light reflection between the two surfaces of a thin-cut slot in a fiber. As the reflectance at the fiber/air or fiber/liquid interface was relatively low (a few percent only), the sensitivity of these devices was not satisfactory.

This work demonstrated that thin silver (Ag) coatings could greatly enhance the interference and the sensitivity of Fabry-Perot etalons for detecting the refractive index of liquids. The greatly enhanced performance is based on the unique optical properties of Ag thin films: 1) low absorption loss in visible spectrum range, and 2) adjustable reflectance/transmittance by varying the film thickness over 10-20 nm. However, Ag films are sensitive to the environment and get oxidized if exposed to air [18], [19]. Furthermore, like most metals, a Ag film exhibits hydrophobic surface and low wettability, which restricts the flow of liquids and limits the use of Ag-based etalon for measuring liquids [20]. On the other hand, a hydrophilic surface could be achieved by using a dielectric or metal oxide layer [21]. The dielectric layer can also protect the Ag film from being oxidized. Hence, our proposed sensors have

Manuscript received June 20, 2017; accepted August 6, 2017. Date of publication August 18, 2017; date of current version October 24, 2017. This work was supported in part by the National Science Foundation under Award 1700785 and Award 1700787 and in part by Sanford Health–South Dakota State University Collaborative Research Seed Grant Program. The associate editor coordinating the review of this paper and approving it for publication was Prof. Venkat R. Bhethanabotla. *(Corresponding author: Qi Hua Fan.)*

N. Uddin and H.-J. Yoon are with the Department of Electrical Engineering and Computer Science, South Dakota State University, Brookings, SD 57007 USA.

M. Shrestha, B. Zheng, and Q. H. Fan are with the Department of Electrical and Computer Engineering and the Department of Chemical Engineering and Materials Science, Michigan State University, East Lansing, MI 48824 USA (e-mail: qfan@egr.msu.edu).

X. Wang is with the Department of Biology and Microbiology, South Dakota State University, Brookings, SD 57007 USA.

Digital Object Identifier 10.1109/JSEN.2017.2741783

the potential to accurately detect the glucose level in blood. In addition, the sensors can also determine the refractive index of hemoglobin. The feasibility of the Fabry-Perot sensors was confirmed by the work of Friebel and Meinke who correlated the glucose levels with the refractive index [22]. Furthermore, Mazarevica et al recently reported that high concentrations of glucose led to an increase of the refractive index of hemoglobin in diabetic patients [23]. Since the refractive index is only sensitive to the compositions of the solutions to be measured, ultrasmall (femtoliter to nanoliter) volume is needed in the analysis [24]. Liaket and Ozana recently demonstrated NIR spectroscopy method for wearable sensor glucose monitoring, which was highly sensitive in identifying specific chemicals in the samples.

This paper presents a Fabry-Perot etalon that combines the advantages of Ag thin films and dielectric coatings described above. Semi-transparent Ag layers were used to reflect the light and produce intensive interference. A thin layer of SiO_2 was deposited onto the Ag to protect it from oxidation and create a super-hydrophilic surface. A prototype sensor included two glass substrates coated with Ag/SiO_2 layers and separated by a spacer to form a cavity of controlled thickness. Transmittance spectra were acquired using a spectrophotometer. The sensors provided high sensitivity and instant response to the change of refractive index of sugar solutions. In addition to measuring glucose level in blood, this sensor has promising potential for detecting various chemicals in liquids for disease diagnosis and waste control.

II. Device Structure and Principle

A basic Fabry-Perot etalon consists of two closely spaced partially reflective surfaces as shown in FIG. 1(a) [25]. When light travels to the reflecting surfaces, part of the light is reflected and part is transmitted. Multiple offset beams interfere with each other. The interference is periodic in wavelength (FIG. 1(b)). Although the transmission and reflection in the proposed modified Fabry-Perot etalon is more complicated, the basic theory discussed here is applicable.

The transmitted wave is the summation of the infinite number of rays from the etalon. The ratio of the total transmitted field to the incident field is

$$\frac{E_{trans}}{E_{inc}} = tt' + tt'r'r'e^{i\delta} + tt'r'^4e^{i2\delta} + tt'r'^6e^{i3\delta} + \ldots = \frac{tt'}{1-r^2e^{i\delta}} = \frac{1-r^2}{1-r^2e^{i\delta}} = \frac{1-\mathbf{R}}{1-\mathbf{R}e^{i\delta}} \quad (1)$$

where r and t are the reflection and transmission coefficients for the light travelling from the air to the medium having refractive index n, respectively. Similarly, for light travelling in the reverse direction, the reflection and transmission coefficients are r' and t', respectively. The reflectance R can be expressed in terms of the coefficient as $R = |r|^2$. The phase δ between two consecutive rays is

$$\delta = \frac{2\pi ndcos\theta}{\lambda} \quad (2)$$

where d is the distance between the two semi-transparent glass substrates, $\theta$is the transmission angle, n is the refractive index of the medium, and λ is the wavelength of the light source.

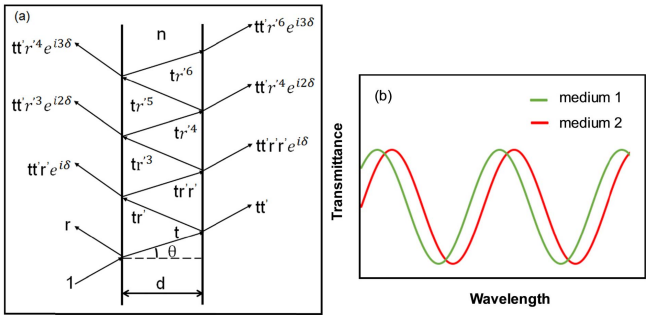

Fig. 1. A basic Fabry-Perot etalon structure (a) and its transmission spectra with two different media (b).

The transmittance, T, is the ratio of the transmitted and incident light intensities

$$T = \frac{(1-\mathbf{R})^2}{1+\mathbf{R}^2-2\mathbf{R}cos2\delta} = \frac{(1-\mathbf{R})^2}{1+\mathbf{R}^2+2\mathbf{R}(1-cos2\delta)} = \frac{(1-\mathbf{R})^2}{(1-\mathbf{R})^2+4\mathbf{R}sin^2\delta} \quad (3)$$

The frequency υ, at which the maximum transmission occurs, is

$$\upsilon = m\frac{c}{2ndcos\theta} \quad (4)$$

where m is an integer which determines the order of the transmission peaks existing in the Fabry-Perot etalon. The separation of the frequency between two consecutive maximum transmission points is known as free spectral range (*FSR*) [26].

$$FSR = \Delta\upsilon = \upsilon_{m+1} - \upsilon_m = \frac{c}{2ndcos\theta} \quad (5)$$

From the transmission spectrum of the Fabry-Perot etalon, the refractive index n of the medium in the cavity or the thickness d of the cavity can be extracted using the equation (5). If a measurement is conducted at normal incident ($\theta = 0$), then $\cos\theta = 1$.

Each sensor can be first calibrated by measuring the transmission spectrum with an air gap, which has a known refractive index of 1. Using Equation (5), the gap thickness d can be deduced from the transmission peak positions. After d is known, a liquid sample with unknown refractive index can be injected into the gap. Measuring the transmittance again will provide another spectrum that has different peak positions as compared with the air gap. Since d will not change, the new peak positions can be used to deduce the refractive index of the liquid.

FIG. 2 shows the sensor structure for the Fabry-Perot etalon proposed in this work. The top and bottom reflection layers were Ag thin films coated on glass slides. The Ag film thickness was about 10-15 nm, which led to very little absorption and allowed sufficient light to pass through the etalon and meanwhile created strong interference. A thin SiO_2 layer ($\sim$ 5 nm) was coated on the Ag films. It greatly increased the hydrophilicity of the surface so that the liquid could easily flow into the cavity. The effects of SiO_2 on various surfaces have been studied in previous works [27]–[30]. The SiO_2 film also protected the Ag film from oxidation and the sensor could

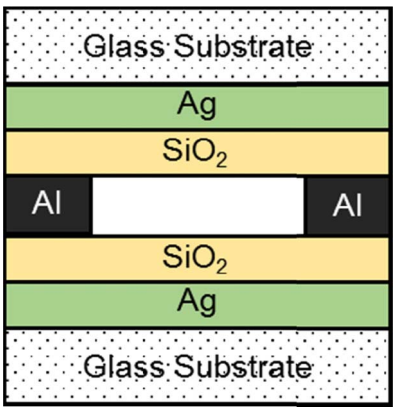

Fig. 2. A modified Fabry-Perot etalon structure.

be washed and reused. Since the SiO_2 layer was very thin, it had little effect on the optical characteristics of the Fabry-Perot sensor, as shown in the result section. An Al film was used as the spacer layer. Although any other films could be used as the spacer, the Al film could be used as electrodes for measuring electric properties in future tests. A larger space or thicker Al film will lead to a transmission spectrum that has more and closer interference peaks according to equation (5).

III. Experimental

A. Substrate Cleaning

Glass microscope slides (Fisherbrand, Economy Plain) were cut into 1.5×1.0 inch^2 substrates for device fabrication. These substrates were soaked in a warm soap solution for 10 minutes to clean off the oils and organic residue. Then the glass substrates were soaked in DI water for 10 minutes. The substrates were then rinsed with the DI water several times followed by ultra-sonication in fresh DI water. The glass substrates were then soaked in acetone for 10 minutes followed by ultra-sonication for 30 minutes. Likewise, the substrates were soaked in isopropanol for 10 minutes followed by ultra-sonication in isopropanol for 30 minutes. The glass substrates were then dried using nitrogen blow prior to silver deposition.

B. Film Deposition and Sugar Solution Preparation

Ag thin films were deposited on the glass substrates using a custom-built RF sputtering system with load-lock chamber. The conditions for the RF sputtering were: base pressure $1 - 2 \times 10^{-6}$ Torr, Ar gas flow 10 sccm, working pressure 3×10^{-3} Torr, RF power 50 W, reflection power 0 W, and deposition time 20 sec. Pre-sputtering of Ag was performed to avoid contamination from the target.

The Ag deposited glass substrates were masked ($3/8 \times 1.5$ inch^2) at the center to protect the active area from Al deposition. The Al spacer layer was deposited using the load-lock RF sputtering system. The base pressure for deposition was $1 - 2 \times 10^{-6}$ Torr. The Ag coated substrates were heated for 10 minutes at 150 °C for better film adhesion prior to sputtering. The working pressure during the deposition was 4 mTorr. The applied RF power and Ar gas flow rate were 75 W and 10 sccm, respectively. The deposition produced Al spacers with thickness of 3-5 μm.

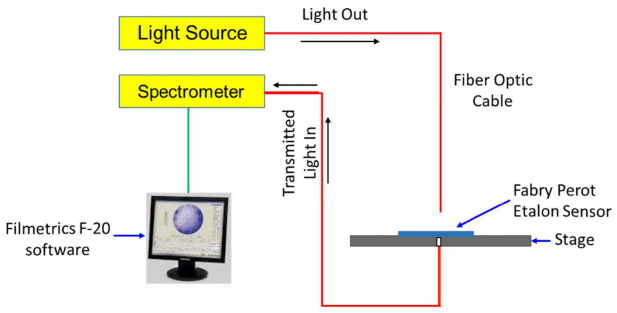

Fig. 3. Optical set up for refractive index measurement.

The SiO_2 thin films was sputtered on top of the Ag-coated glass substrates. The deposition conditions were: RF power 50 W, Ar gas flow rate 10 sccm, pressure 4 mTorr, and deposition time 3 min. The thickness of the SiO_2 layer was $\sim$ 5 nm, which was deduced from a much longer deposition (e.g. two hours) using the same parameters.

The sugar solutions were prepared per the brix content of sugar. The sugar solutions with concentration of 2%, 5%, 7%, 10%, and 20% were prepared by adding 0.4 gm, 1 gm, 1.4 gm, 2 gm, and 4gm sugar in 20 ml DI water, respectively.

C. Sample Measurement and Optical Modeling

The film thickness was measured using a Dektak 150 profilometer. The deposition rates for the films were derived from longer depositions, assuming the film thickness varied linearly with the deposition time. The optical transmittance was measured using a Filmetrics F20-UVX spectrophotometer. The optical modeling was performed using a Macleod Thin Film software.

D. Optical Set Up

Optical transmittance of the Fabry Perot etalon sensors was measured using a Filmetrics F-20 spectrophotometer (wavelength range 190-1700 nm) with Hamamatsu (L120290) light source. The system configuration is shown in FIG. 3. The light source was turned ON for over 15 minutes before the measurements. Filmetrics F-20 software was used to investigate the spectra. The system was calibrated for 100% and 0% transmittance by removing any sample on the stage and placing an opaque sample on the stage, respectively. Then the interested sample was placed on the stage and measurement was taken from the software.

IV. Result and Discussion

FIG. 4 shows the simulated transmittance spectra of a Fabry-Perot etalon illustrated in FIG. 2. The Ag film was 15 nm thick, the SiO_2 layer was 5 nm thick, and the air gap was 3 μm thick. The continuous line (green color) was the spectrum with 5 nm SiO_2 films and the dotted line (red color) was the spectrum with the SiO_2 films replaced with equivalent air. This result confirmed that the peak shift induced by the thin SiO_2 layer was almost negligible.

The surface wettability of the Ag-coated glass substrates was evaluated using a contact angle measurement. FIG. 5 indicated a hydrophobic surface of the Ag layer. The left and

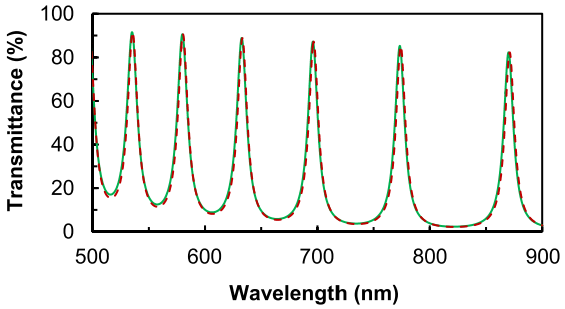

Fig. 4. Transmittance spectra of a modified Fabry-Perot etalon illustrated in FIG. 2. Continuous line (green): with SiO_2 thin layers of 5 nm thick. Dotted line (red): with the SiO_2 layers replaced with equivalent air.

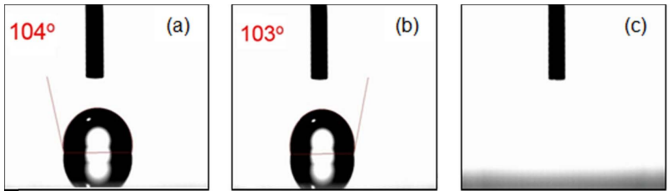

Fig. 5. Silver surface contact angles (a, b), and a completely wetted SiO_2 coated surface (c).

right contact angle of the Ag surface was 104° and 103°, respectively, which didn't allow liquid to flow easily in the Ag surface. With the SiO_2 layer on top of the Ag, the water drop spread out immediately and could not be measured. The super-hydrophilic SiO_2 surface allowed the sugar solutions to completely fill the cavity between the two SiO_2/Ag coated slides spaced with the Al layer.

Sugar solutions with brix concentration from 2% to 20% were measured. Each solution was measured using a different sensor to ensure no cross-contamination. The transmission spectra with air and a sugar solution in the gap were measured and used to determine the gap thickness and the refractive index of the liquid, respectively. First, using two consecutive interference peaks with an air gap (refractive index 1.000), the gap thickness was first determined. Using the gap thickness and two corresponding peaks in the transmission spectrum of a sugar solution, the refractive index of the liquid was subsequently calculated. The wavelength in which the refractive index was calculated was around 590 nm.

As an example, FIG. 6a shows the transmission spectra of a sensor with an air gap and 2% sugar solution, respectively. With an air gap, two consecutive interference peaks were found at 591.63 nm and 647.91 nm, which led to a gap thickness of 3.40 μm. With the 2% sugar filling in the gap, two interference peaks were found at 570.70 nm and 608.84 nm, from which the refractive index was deduced to be 1.337.

The transmission spectra of the 5%, 7%, 10%, and 20% solutions are shown in FIG. 6(b)-6(e), each being measured with an air gap and a sugar-solution-filled gap, respectively. The gap thickness and refractive indices of the sugar solutions were determined in a similar way as the 2% sugar solution discussed above. Table I summarizes the peak positions, calculated gap thickness, and refractive indices.

The refractive index of 5% sugar solution was measured at different temperatures. The refractive index was found

TABLE I

SUMMARY OF THE PEAK POSITIONS IN THE TRANSMISSION SPECTRA WITH AIR GAP AND SUGAR-SOLUTION-FILLED GAP, CALCULATED GAP THICKNESSES, AND REFRACTIVE INDICES

Sugar soluti -on	Air gap			Solution gap		
	Peak 1 (nm)	Peak 2 (nm)	Gap thick. (μm)	Peak 1 (nm)	Peak 2 (nm)	n
2%	591.63	647.91	3.40	570.70	608.84	1.337
5%	568.37	604.19	4.79	585.12	613.02	1.341
7%	570.23	606.05	4.82	587.91	615.81	1.344
10%	558.60	595.35	4.52	579.53	608.37	1.350
20%	585.12	619.07	5.33	592.08	617.17	1.365

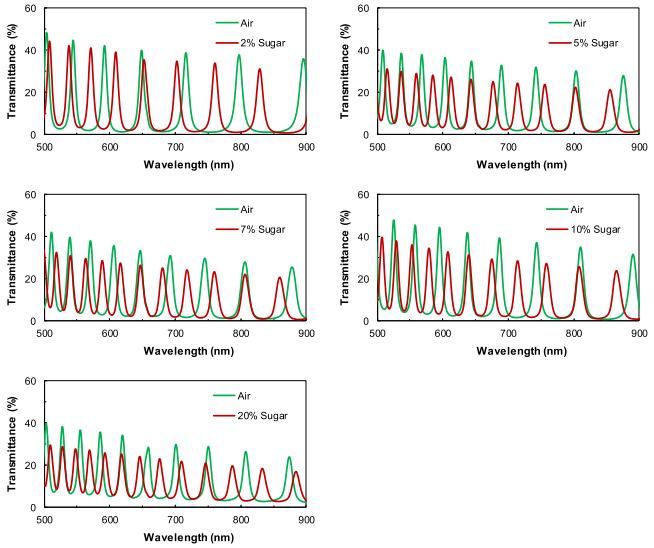

Fig. 6. Transmission spectra of the Fabry-Perot etalons with air gap and sugar-solution-filled gap: (a) 2% sugar solution, (b) 5% sugar solution, (c) 7% sugar solution, (d) 10% sugar solution, and (e) 20% sugar solution.

to be 1.340, 1.338, 1.336 and 1.334 at 24.7 °C, 35.3 °C, 50.7 °C and 65.6 °C, respectively, with a reference wavelength of $\sim$ 600 nm. Thus, the refractive index was inversely proportional to temperature at a rate of .00014/°C, as shown in FIG. 7. This temperature effect was attributed mainly to the decrease in the density of the solution with increasing temperature.

The refractive index vs. the brix concentration was plotted in FIG. 6, which shows a linear response. Using this linear relationship, the sugar concentration in water solution can be extracted from the value of refractive index. For an unknown sugar solution, after measuring the refractive index using this Fabry-Perot etalon, the brix percentage can be readily derived from the fitting equation given in FIG. 6. The sensitivity of this measurement is reflected by the slope of the linear fitting, being 1.7×10^{-3} refractive index per brix%. This sensitivity can be translated into wavelength difference using equation (5). Assuming the center wavelength between the two transmission peaks is 600 nm and the sensor has a gap of 500 nm thick, then a change of $\sim 1.7 \times 10^{-3}$ in the refractive index will lead to a variation of 0.34 nm in the wavelength difference between the two transmission peaks. This variation

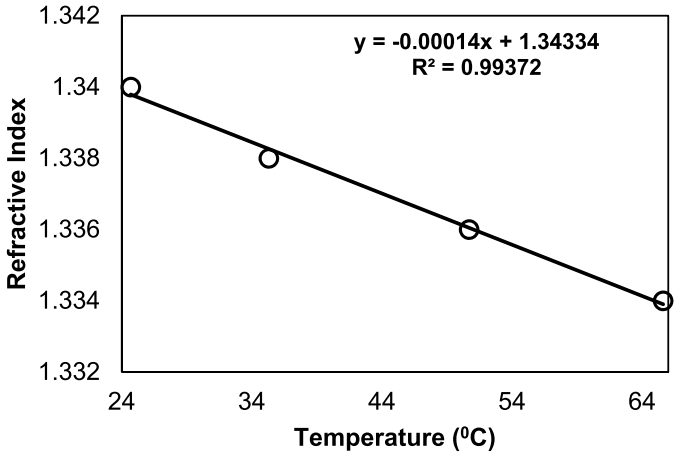

Fig. 7. Refractive index vs temperature for 5% sugar solution.

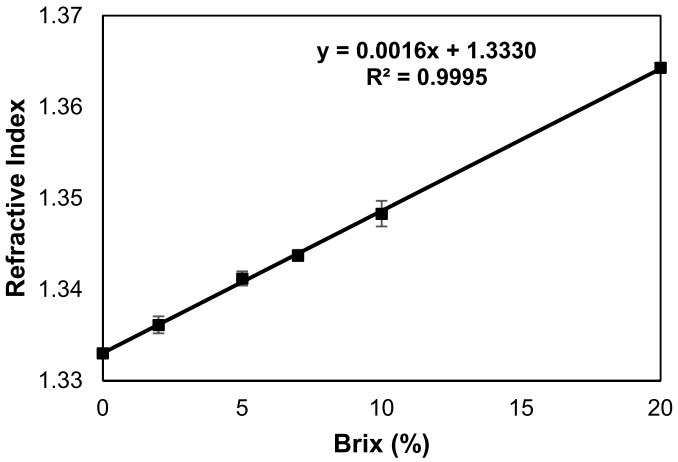

Fig. 8. Refractive index vs. brix (%) concentration. Rectangle: measured values. Continuous line: fitting result.

in wavelength can be readily detected using the spectrophotometer. The smallest concentration difference that can be determined by the Fabry-Perot sensor is ~ 0.05 brix% which is same as compared with the other approaches mentioned in references [31], [32]. The resolution of the concentration was found from the sensitivity and resolution of the refractive index which is 10^{-4} refractive index unit. As discussed before, the sensors measure the positions of the interference peaks. Therefore, the signal-to-noise ratio (SNR) depends on the resolution of the spectrophotometer. The maximum resolution of spectrophotometer in determining the peak wavelength is 0.1 Åor 0.01 nm. The uncertainty in the measurement of peak position in the interference spectrum will be considered as noise. This noise in determining the peak wavelength can be related to the uncertainty of the refractive index. The refractive index (n) of 1.337 was found for 2% sugar solution using the peak interference wavelength of transmittance spectrum given in Table I. The refractive index difference (Δn) of $4.5*10^{-5}$ was found due to the uncertainty in determining the peak positions from the transmittance spectrum. The SNR was found to be 54.69 dB, which was comparable or better than the other sensors available for detect the liquid/gas levels (50 dB in [33], 31.22 dB in [34] or 25 dB in [35]).

TABLE II
COMPARISON OF THE REPORTED AND EXPERIMENTAL RESULTS

Brix percentage	Refractive index reported	Refractive index measured(average)	Difference/measured ×100%
2	1.335	1.336	.075
5	1.340	1.341	.076
7	1.343	1.343	0
10	1.347	1.348	.074
20	1.363	1.364	.073

Table II compares our experimental results with the reported refractive indices of sugar solutions [36]. All the four measurements were in good agreement. Therefore, the Fabry-Perot etalon had excellent accuracy.

V. CONCLUSION

A Fabry-Perot etalon using two semi-transparent Ag/SiO_2 surfaces is highly accurate in determining the refractive indices of sugar solutions. The SiO_2 film not only protects the reflective Ag layer, but also provides a superhydrophilic surface that allows liquid to easily flow into the cavity. The refractive index is linearly proportional to the sugar concentration. This sensor has the potential to accurately detect specific chemical species in liquids.

REFERENCES

[1] P. Domachuk, I. Littler, M. Cronin-Golomb, and B. Eggleton, "Compact resonant integrated microfluidic refractometer," *Appl. Phys. Lett.*, vol. 88, no. 9, p. 093513, 2006.
[2] T. Koschinsky and L. Heinemann, "Sensors for glucose monitoring: Technical and clinical aspects," *Diabetes/Metabolism Res. Rev.*, vol. 17, no. 2, pp. 113–123, 2001.
[3] J. S. Maier, S. A. Walker, S. Fantini, M. A. Franceschini, and E. Gratton, "Possible correlation between blood glucose concentration and the reduced scattering coefficient of tissues in the near infrared," *Opt. Lett.*, vol. 19, no. 24, pp. 2062–2064, 1994.
[4] J. H. Chong, P. Shum, H. Haryono, A. Yohana, M. K. Rao, C. Lu, and Y. Zhu, "Measurements of refractive index sensitivity using long-period grating refractometer," *Opt. Commun.*, vol. 229, pp. 65–69, 2004.
[5] W. M. Yunus and A. B. Rahman, "Refractive index of solutions at high concentrations," *Appl. Opt.*, vol. 27, no. 16, pp. 3341–3343, 1988.
[6] A. Paliwal, A. Sharma, M. Tomar, and V. Gupta, "Long range surface plasmon resonance (LRSPR) based highly sensitive refractive index sensor using Kretschmann prism coupling arrangement," in *Proc. AIP Conf.*, 2016, p. 020132.
[7] A. Marzuki and N. W. Sari, "Design of reflective optical fiber sensor for determining refractive index and sugar concentration of aqueous solutions," *Mater. Sci. Eng.*, vol. 107, no. 1, p. 012032, 2016.
[8] M. V. Hernández-Arriaga, M. A. Bello-Jiménez, A. Rodríguez-Cobos, and M. V. Andrés, "Experimental investigation of fused biconical fiber couplers for measuring refractive index changes in aqueous solutions," *IEEE Sensors J.*, vol. 16, no. 1, pp. 132–136, Jan. 2016.
[9] C. Liu *et al.*, "Fibre optic chemical sensor based on graphene oxide-coated long period grating," in *Proc. 6th Eur. Workshop Opt. Fibre Sens.*, 2016, p. 99160V.
[10] M. C. Shih, H.-H. Yang, and C. H. Shih, "Measurement of the index of refraction of an liquid by a cladding depleted fiber Bragg grating," *Opt. Quantum Electron.*, vol. 48, pp. 1–6, Feb. 2016.
[11] X. Liu, Z. Cao, Q. Shen, and S. Huang, "Optical sensor based on Fabry-Pérot resonance modes," *Appl. Opt.*, vol. 42, no. 36, pp. 7137–7140, 2003.
[12] Z.-M. Qi, I. Honma, and H. Zhou, "Nanoporous leaky waveguide based chemical and biological sensors with broadband spectroscopy," *Appl. Phys. Lett.*, vol. 90, no. 1, p. 011102, 2007.

[13] L. S. Live, M.-P. Murray-Méthot, and J.-F. Masson, "Localized and propagating surface plasmons in gold particles of near-micron size," *J. Phys. Chem. C*, vol. 113, no. 1, pp. 40–44, 2008.
[14] Z. L. Ran, Y. J. Rao, W. J. Liu, X. Liao, and K. S. Chiang, "Laser-micromachined Fabry-Pérot optical fiber tip sensor for high-resolution temperature-independent measurement of refractive index," *Opt. Exp.*, vol. 16, no. 3, pp. 2252–2263, 2008.
[15] D. Majchrowicz, M. Hirsch, P. Wierzba, M. Bechelany, R. Viter, and M. Jędrzejewska-Szczerska, "Application of thin ZnO ALD layers in fiber-optic Fabry-Pérot sensing interferometers," *Sensors*, vol. 16, no. 3, p. 416, 2016.
[16] V. Bhatia *et al.*, "Optical fibre based absolute extrinsic Fabry-Pérot interferometric sensing system," *Meas. Sci. Technol.*, vol. 7, no. 1, p. 58, 1996.
[17] K. A. Murphy, M. F. Gunther, A. M. Vengsarkar, and R. O. Claus, "Quadrature phase-shifted, extrinsic Fabry-Pérot optical fiber sensors," *Opt. Lett.*, vol. 16, no. 4, pp. 273–275, 1991.
[18] H. Jaeger, P. D. Mercer, and R. G. Sherwood, "The effect of exposure to air on silver and gold films deposited in ultra-high vacuum," *Surf. Sci.*, vol. 13, no. 2, pp. 349–360, 1969.
[19] L. A. A. Pettersson and P. G. Snyder, "Preparation and characterization of oxidized silver thin films," *Thin Solid Films*, vol. 270, pp. 69–72, Dec. 1995.
[20] R. A. Erb, "Wettability of metals under continuous condensing conditions," *J. Phys. Chem.*, vol. 69, no. 4, pp. 1306–1309, 1965.
[21] S. Sankar *et al.*, "Hydrophobic and metallophobic surfaces: Highly stable nonwetting inorganic surfaces based on lanthanum phosphate nanorods," *Sci. Rep.*, vol. 6, p. 1, Apr. 2016.
[22] M. Friebel and M. Meinke, "Model function to calculate the refractive index of native hemoglobin in the wavelength range of 250–1100 nm dependent on concentration," *Appl. Opt.*, vol. 45, no. 12, pp. 2838–2842, 2006.
[23] O. Sydoruk, O. Zhernovaya, V. Tuchin, and A. Douplik, "Refractive index of solutions of human hemoglobin from the near-infrared to the ultraviolet range: Kramers-Kronig analysis," *J. Biomed. Opt.*, vol. 17, no. 11, p. 115002, 2012.
[24] X. Fan, I. M. White, S. I. Shopova, H. Zhu, J. D. Suter, and Y. Sun, "Sensitive optical biosensors for unlabeled targets: A review," *Anal. Chimica Acta*, vol. 620, nos. 1–2, pp. 8–26, Jul. 2008.
[25] G. Hernandez, *Fabry-Pérot Interferometers*. Cambridge, U.K.: Cambridge Univ. Press, 1988.
[26] M. Vaughan, *The Fabry-Pérot Interferometer: History, Theory, Practice and Applications*. Boca Raton, FL, USA: CRC Press, 1989.
[27] M. Machida, K. Norimoto, T. Watanabe, K. Hashimoto, and A. Fujishima, "The effect of SiO_2 addition in super-hydrophilic property of TiO_2 photocatalyst," *J. Mater. Sci.*, vol. 34, no. 11, pp. 2569–2574, 1999.
[28] J. Yu, X. Zhao, C. Y. Jimmy, G. Zhong, J. Han, and Q. Zhao, "The grain size and surface hydroxyl content of super-hydrophilic TiO_2/SiO_2 composite nanometer thin films," *J. Mater. Sci. Lett.*, vol. 20, no. 18, pp. 1745–1748, 2001.
[29] V. Masteika, J. Kowal, N. S. J. Braithwaite, and T. Rogers, "A review of hydrophilic silicon wafer bonding," *ECS J. Solid State Sci. Technol.*, vol. 3, no. 4, pp. Q42–Q54, 2014.
[30] T. Suni, K. Henttinen, I. Suni, and J. Mäkinen, "Effects of plasma activation on hydrophilic bonding of Si and SiO_2," *J. Electrochem. Soc.*, vol. 149, no. 6, pp. G348–G351, 2002.
[31] H. Sobral and M. Peña-Gomar, "Determination of the refractive index of glucose-ethanol-water mixtures using spectroscopic refractometry near the critical angle," *Appl. Opt.*, vol. 54, no. 28, pp. 8453–8458, 2015.
[32] A. Crespi *et al.*, "Three-dimensional Mach-Zehnder interferometer in a microfluidic chip for spatially-resolved label-free detection," *Lab a Chip*, vol. 10, no. 9, pp. 1167–1173, 2010.
[33] D. K. C. Wu, B. T. Kuhlmey, and B. J. Eggleton, "Ultrasensitive photonic crystal fiber refractive index sensor," *Opt. Lett.*, vol. 34, no. 3, pp. 322–324, Feb. 2009.
[34] W. Zhang *et al.*, "An optical fiber Fabry-Pérot interferometric sensor based on functionalized diaphragm for ultrasound detection and imaging," *IEEE Photon. J.*, vol. 9, no. 3, Jun. 2017, Art. no. 7103208.
[35] Y. Ou *et al.*, "Method of hybrid multiplexing for fiber-optic Fabry–Pérot sensors utilizing frequency-shifted interferometry," *Appl. Opt.*, vol. 53, no. 35, pp. 8358–8365, 2014.
[36] A. Armstrong, J. Blatt, J. Grantham, D. Higley, K. Luginbuhl, and K. Nienburg, "Lab-on-a-chip diagnostic biosensor," Colorado State Univ., Fort Collins, CO, USA, Tech. Rep., 2011.

Nezam Uddin was born in Dhaka, Bangladesh, in 1990. He received the B.Sc. degree in electrical and electronic engineering from the Khulna University of Engineering and Technology in 2012 and the M.S. degree in electrical engineering and computer science from South Dakota State University (SDSU), USA, in 2017. He is currently pursuing the Ph.D. degree in electrical and computer engineering from the University of Nebraska–Lincoln, NE, USA.

From 2015 to 2017, he was a Research and Teaching Assistant with the Electrical Engineering Department, SDSU. His research interests include simulation, fabrication and characterization of semiconductor low-dimensional electronic, micro/nano photonics, bio-entities interaction of light with nanostructures, thin film optics, fiber-optic sensing/actuation devices and systems. He has been awarded a 2017 Optics and Photonics Education Scholarship by SPIE, the International Society for Optics and Photonics, for his potential contributions to the field of optics, photonics or related field.

Maheshwar Shrestha received the B.E. degree in electronics and communication engineering from Pokhara University, Nepal, in 2004, the M.S. and Ph.D. degrees in electrical engineering from South Dakota State University, Brookings, SD, in 2012 and 2015 respectively.

From 2004 to 2009, he was a Lecturer with Purbanchal University affiliated colleges in Nepal. From 2015 to 2016, he was a Post-Doctoral Fellow with the Electrical Engineering and Computer Science Department, South Dakota State University. Since 2016, he has been a Post-Doctoral Fellow with the Electrical and Computer Engineering Department, Michigan State University, East Lansing, MI. His research interests include nanomaterials, nanostructures, and thin films for application in energy conversion, energy storage, and optoelectronics devices.

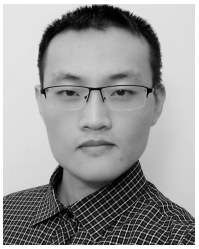

Bocong Zheng received the Ph.D. degree in surface engineering from the Dalian University of Technology, China, in 2016. He is currently undertaking post-doctoral research at Michigan State University. His current research focuses on the simulation of low temperature plasmas, including capacitively and inductively coupled plasmas, plasma-liquid interactions and magnetron sputtering discharges.

Hyeun-Joong Yoon received the B.S., M.S., and Ph.D. degrees in electrical engineering from Ajou University, South Korea, in 1999, 2001, and 2007, respectively. Between 2003 and 2006, he was a Display Circuit System Engineer with the Research and Development Center, Hydis, a TFT-LCD manufacture company in South Korea. He was a Post-Doctoral Research Fellow with the Department of Chemical Engineering, University of Michigan, between 2010 and 2015. He is currently an Assistant Professor with the Department of Electrical Engineering and Computer Science, South Dakota State University. His current research is to create cutting edge engineering solutions to clinical problems with novel translational biomedical research tools.

Xiuqing Wang received the Ph.D. degree in virology/pathobiology from the University of Connecticut in 2000. She did postdoctoral work in Dr. S. Dewhurst's Laboratory, Department of Microbiology and Immunology, University of Rochester Medical Center. She has worked on infectious bronchitis virus (a prototype of Coronavirus), human immunodeficiency virus-1 (HIV-1), human herpesvirus-6, murine cytomegalovirus, porcine reproductive and respiratory syndrome virus (PRRSV), and porcine epidemic diarrhea virus (PEDV). More recently, her laboratory is interested in uncovering the role of host's innate immunity in virus infections. In collaboration with Dr. J. White at the Sanford Health and Dr. S.-Y. Marzano at South Dakota State University, she initiated a new research project to map the human gut virome in the breast- and formula-fed preterm infants. Her primary research interests are focused on viral pathogenesis, viral immunity, and vaccine development.

Qi Hua Fan received the Ph.D. degree in applied physics from the University of Aveiro in 1999. He is currently an Associate Professor with Michigan State University. His research interest includes plasma sources for large-area coatings and plasma processing of nanostructured materials for energy harvesting, energy storage, and electro-optical devices.